A study on the representation of local effects in low-order models for thin-walled rod members

Marcos P. Kassab[1], Eduardo M. B. Campello[1], Adnan Ibrahimbegovic[2,3]

[1]*Dept. of Structural and Geotechnical Engineering, Polytechnic School, University of São Paulo*
P.O. Box 61548, 05424-970, São Paulo, SP, Brazil
marcos.kassab@usp.br, campello@usp.br
[2]*University of Technology Compiègne - Alliance Sorbonne University, Laboratoire Roberval, Centre de recherche Royallieu, rue de docteur Schweitzer, Compiégne, 60200, Hauts-de-France, France*
[3]*Institut Universitaire de France, 75005, 1 rue Descartes, Paris, France*
adnan.ibrahimbegovic@utc.fr

Abstract. This work aims to explore alternatives to represent local effects, such as local buckling and plasticity, in low order models of thin-walled rod members. The discussion is carried out on a theoretical-numerical level, and a few illustrative examples are provided. The techniques that are explored stem from two different approaches: (i) direct enrichment of the rod kinematics and (ii) multiscale methods. Direct enrichment of low order kinematics usually leads to models with optimal computational cost, while still at the downside of having lower-order (still limited) kinematics. Models derived from the Generalized Beam Theory (GBT) are an example of such an approach. Multiscale methods, in turn, rely on results of higher-order theories (e.g., shells and 3D solids) to improve the performance of the lower-order model. The associated computational cost and accuracy vary widely with the imposed coupling level between the different scales. It is possible to have models ranging from full coupling at run-time – the so-called strong coupling multiscale method – to no coupling at all – the higher-order models are used only to compute meaningful mechanical quantities that are passed on to the low order model at some point. The work is an on-going development of a PhD research by the first author, and the provided results are partial.

Keywords: Thin-walled rods; local buckling; reduced order model.

1 Introduction

In real-life applications, computation time constraints play a major role in the numerical representation of mechanical processes. In an attempt to limit computational costs, low-order or reduced-order models (ROMs) can be employed, given that the most important aspects of the analyzed problem are usually captured. Structural engineers are used to recur to ROMs in daily design practice, since the so-called structural theories (truss, beam, plates, shells, etc.) are a simplification of the complete continuum mechanics: from 3D solid mechanics, kinematical and material assumptions are imposed, thus conveniently reducing the dimensionality of the problem, whilst limiting to some extent prevision capabilities.

However, for the increasingly challenging tasks proposed by modern engineering, traditional simplified models often no longer suffice to produce the desired accuracy and safety level, forcing research teams to develop more robust (hierarchically superior) models. A wide array of options are available to improve existing models: a) abandon some of the assumptions and increase the problem dimensionality (e.g., go from rod models to plate/shell models or from plate/shell to 3D-solid models); b) weaken the constraints of the kinematical and material assumptions (e.g., allow torsional warping in rods, material anisotropy or inelasticity, etc); c) employ refined

models to generate high-fidelity simulations, then extract relevant information of the phenomenon of interest and represent it in terms of ROM degrees-of-freedom (DOFs) (e.g., multiscale and multiscale-like techniques).

In the case of 3D frame structures consisted of thin-walled members, modeling local effects (such as those arising from cross-sectional distortion, from either material or geometrical causes) is particularly intricate, since there is an explicit violation of the usual rigid cross-section assumption. Moreover, for steel or aluminum members, inelastic behavior is often present and the coupling among local geometrical and material effects is a common scenario. Also, it is a source of concern in structural design, since this kind of phenomenon can dictate the load bearing capacity of the member.

In this work, we present some recent developments of an ongoing research about the incorporation of such local effects within a ROM (rod) framework. We intend to explore alternatives to robustly estimate critical/ultimate loads (including plastic behavior) and compute the full equilibrium path of the structure, even when far from initial configurations, while also pointing out aspects that are under development and needing further exploration.

2 Kinematically exact rod model with torsional warping DOFs and polyconvex hyperelastic constitutive equation

Three-dimensional kinematically exact rod models have been in development for the past four or five decades and have reached a significant level of maturity. One should mention the pioneering works from Simo and Vu-Quoc [1], [2], studies on finite rotations from Ibrahimbegovic and Frey [3], [4], correction of Simo's work from Pimenta and Yojo [5], inclusion of torsion warping from Pimenta and Campello [6], introduction of advanced hyperelastic constitutive equations from Campello and Lago [7], and the more recent work from Kassab and Campello [8]. It is also worth mentioning the kinematically exact Bernoulli-Euler-like rod theory from Pimenta and Silva et al. [9]. Other relevant works, that follow similar developments, but differ on some theoretical choices (e.g. rotation parametrization, construction of warping function, conjugated stress-strain pairs, etc) should be cited, such as Crisfield [10], Gruttman et al [11], [12] and Gonçalves [13], to cite just a few. The geometrical exactness of this kind of model follows fig. 1a).

Given an initial reference system $\{\boldsymbol{e}_1^r, \boldsymbol{e}_2^r, \boldsymbol{e}_3^r\}$, where $< \boldsymbol{e}_1^r, \boldsymbol{e}_2^r >$ spans the cross-sectional reference plane and $\boldsymbol{e}_3^r$ is the axial direction, and a current reference system $\{\boldsymbol{e}_1, \boldsymbol{e}_2, \boldsymbol{e}_3\}$, one can define the initial $\boldsymbol{\xi}$ and current $\boldsymbol{x}$ configurations as

$$\boldsymbol{\xi} = \boldsymbol{a}^r + \boldsymbol{\zeta}, \quad \boldsymbol{x} = \boldsymbol{\zeta} + \boldsymbol{u} + \boldsymbol{Q}\boldsymbol{a}^r + \boldsymbol{w} \tag{1}$$

where $\boldsymbol{a}^r = \xi_\alpha \boldsymbol{e}_\alpha^r$ is the coordinate of cross-sectional points, $\boldsymbol{\zeta} = \zeta \boldsymbol{e}_3^r$ is the axial coordinate, $\boldsymbol{u}$ is the axial displacement, $\boldsymbol{Q}(\boldsymbol{\theta})$ is the cross-sectional rotation tensor, parametrized by the Euler-Rodrigues formula, and $\boldsymbol{w} = p\psi\boldsymbol{e}_3$ is the warping displacements, with shape function ψ and intensity p, and $\boldsymbol{e}_i = \boldsymbol{Q}\boldsymbol{e}_i^r$. One can define frame-invariant generalized back-rotated stress and strain conjugated pairs. In e.g. Kassab and Campello [8] one can find the explicit expression for $\boldsymbol{\eta}^r$ (shear and axial strains), $\boldsymbol{\kappa}^r$ (bending and torsion curvatures), p and p', which are respectively conjugated to $\boldsymbol{n}^r$ (shear and normal forces), $\boldsymbol{m}^r$ (bending and torsion moments), Q (bi-shear) and B (bi-moment). It is convenient to define the generalized displacement, strain and stress vectors $\boldsymbol{d} = [\boldsymbol{u}\ \ \boldsymbol{\theta}\ \ p]^T$, $\boldsymbol{\varepsilon}^r = [\boldsymbol{\eta}^r\ \ \boldsymbol{\kappa}^r\ \ p\ \ p']^T$ and $\boldsymbol{\sigma}^r = [\boldsymbol{n}^r\ \ \boldsymbol{m}^r\ \ Q\ \ B]^T$. One can write the weak form of the equilibrium equations and its linearization in terms of $\boldsymbol{d}, \boldsymbol{\varepsilon}^r, \boldsymbol{\sigma}^r$ and their virtual counterparts (see [8] for the complete expressions). The last missing ingredient in this context is the constitutive equation. Assuming that the material is hyperelastic, there is a potential function $\Psi^e = \Psi^e(\boldsymbol{\varepsilon}^r)$ so that

$$\boldsymbol{\sigma}^r = \frac{\partial \Psi^e}{\partial \boldsymbol{\varepsilon}^r}, \quad \boldsymbol{D} = \frac{\partial^2 \Psi^e}{\partial \boldsymbol{\varepsilon}^{r2}} \tag{2}$$

where $\boldsymbol{D}$ is the material tangent stiffness matrix. In practice, it is shown in Campello and Kassab [8] and Dasambiagio et al.[8], [14] that one can take any hyperelastic material defined in terms of the second Piola-Kirchoff stress tensor and the invariants of right Cauchy-Green strain tensor, and perform appropriate cross-sectional integration to arrive at cross-sectional resultants. A usual choice is a linear elastic relation, or truncated versions of finite strain materials (such as Saint-Venant's and Simo-Ciarlet's materials). However, as shown in Campello and Lago [7] and Campello and Kassab [7], [8], this simplistic choice does not allow for correct strain coupling, and buckling modes featuring coupled compression, torsion and warping strains are usually not detected,

and post-buckling equilibrium path is usually wrong. To correct this, Kassab and Campello employed the complete (i.e., non-truncated) version of Saint-Venant's and Simo-Ciarlet's materials, obtaining very good results for complex cases. Of course, the aforementioned model is blind to local effects such as web/flange buckling and plasticity, but it provides a solid foundation to elastic instability, from which further developments can be carried out.

3 GBT-based enrichment of kinematical assumptions

The first strategy to be explored here consists in taking eq. (1) and allowing a more comprehensive kinematics. Within the author's research group, Pimenta and Campello [15] and Dasmbiagio et al. [14] have already explored how to include additional deformation modes to allow for cross-section deformation. For thin-walled rods, another possible approach is to extend the Generalized Beam Theory (GBT) from Schardt [16] to the fully kinematically exact context. It should be mentioned the efforts from Gonçalves et al. [17], that have already published works in this direction. Despite the great results achieved, the employed constitutive equations are truncated versions of the Saint-Venant's material, associated to a simplified description of secondary (through wall thickness) shell bending rotation. As discussed in section 2 this can have a destructive effect on the capacity of correctly coupling strain terms, leading to incorrect determination of critical load and post-critical paths. Thus, we are developing an alternative formulation that will allow the local shell bending rotation to be calculated according to finite rotation Kirchoff-Love shell theories, using as parameters only rod DOFs (see fig. 1b)). This yields a new expression for the current configuration as follows

$$\boldsymbol{x} = \boldsymbol{x} = \boldsymbol{x}^m + \boldsymbol{x}^h, \text{ with } \boldsymbol{x}^m = \boldsymbol{\zeta} + \boldsymbol{u} + \boldsymbol{y}^m, \ \boldsymbol{x}^h = \boldsymbol{h} \tag{3}$$

where $\boldsymbol{y}^m = \boldsymbol{a}^m + \boldsymbol{v}^m + \boldsymbol{w}^m$ is the cross-sectional mid-line displacement, with rotation $\boldsymbol{a}^m = \boldsymbol{Q}\boldsymbol{a}^{m^r}$, in and out-of-plane distortions given by linear combinations of the in- and out-of-plane displacement modes $\boldsymbol{\phi}_\beta$ and $\boldsymbol{\psi}$, respectively, and associated amplitudes $\boldsymbol{r}$ and $\boldsymbol{p}$, yielding $\boldsymbol{v}^m = (\boldsymbol{\phi}_\beta \cdot \boldsymbol{r})\boldsymbol{e}_\beta$ and $\boldsymbol{w}^m = (\boldsymbol{\psi} \cdot \boldsymbol{p})\boldsymbol{e}_3$, and secondary shell-bending rotation $\boldsymbol{h} = \boldsymbol{Q}^h\boldsymbol{h}^r$, with $\boldsymbol{Q}^h = \boldsymbol{Q}^h(\boldsymbol{u}, \boldsymbol{\theta}, \boldsymbol{p}, \boldsymbol{r})$. The process of defining cross-sectional shape functions can be taken as an adaptation of the one from GBTUL [18], with a post-process stage to separate pure in- from out-of plane modes.

The weak form of the equilibrium and its linearization can be written as a function of $(\boldsymbol{u}, \boldsymbol{\theta}, \boldsymbol{p}, \boldsymbol{r})$, which are rod-level degrees of freedom, characterizing the 1D nature of the proposed formulation. The full expression for the residual and tangent stiffness will not be presented here since this is a work in progress, and adjustments are expected to occur during the process. It can be said for now that, as consequence of eq. (3), the strain field can be additively decomposed in *mid-line* and *out-of-mid-line (shell-bending)* terms, and new stress resultants, conjugated to $\boldsymbol{\eta}^r, \boldsymbol{\eta}^{r\prime}, \boldsymbol{\kappa}^r, \boldsymbol{\kappa}^{r\prime}, \boldsymbol{p}, \boldsymbol{p}', \boldsymbol{p}'', \boldsymbol{r}, \boldsymbol{r}', \boldsymbol{r}''$, shall be defined. To formulate and implement this model in a hyperelastic context is the main goal of the first author's PhD research. It is expected that local buckling effects will be inherently represented, along with the global buckling behaviour (already enabled). This is a challenging task, with good prognostics and has been discussed in Cilamce-2023 (proceedings not yet available).

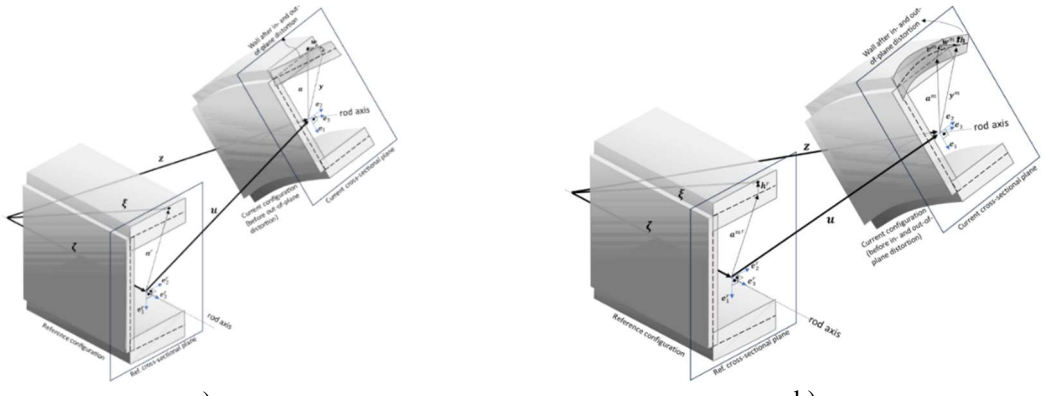

a) b)

Figure 1. Kinematics of rod with cross-sectional rigid-body motion and a) torsional warping only; b), in- and out-of plane distortion.

4 Multiscale techniques

Given the complex nature of finite-displacement theories, and the difficulties of representing local geometric and material (e.g., plastic) effects directly in rod formulations, one promising framework is multiscale and multiscale-like modelling. This approach allows for more robust calculations in a finer (micro) level, that are then transported to the macro-level, which is in general the one of interest of engineering applications. Many developments are possible, and in this section we will discuss how some of them can be applied to thin-walled rod members.

4.1 Parameter inference of constitutive parameters

The simplest technique is a multiscale-like approach assuming at the macro (rod model) level a pre-fixed function for material law, building the representation of the "micro"-level (a finer 3D-solid or shell model) for one rod element, and applying various boundary conditions. Then, match material parameters from the macro-scale material law to the ones measured in this set of micro-scale simulations. A framework for hardening-softening elastoplastic rods, accounting for local effects was idealized by Dujc et al. [19] for the small-strain 2D case, extended to finite strain softening rods in Ibrahimbegovic et al. [20] and Ljukovac et al. [21]. We have adapted it further to the elastoplastic hardening case of 3D rods with torsional warping, operating at macro-level with only cross-sectional stress-resultants. This work is under submission to an archival journal, thus cannot be referenced here yet. In summary, one has an additive decomposition of the free energy function in an elastic and a hardening-plastic part $\Psi(\boldsymbol{\varepsilon}^{re}, \boldsymbol{\xi}^h) = \Psi^{\mathrm{e}}(\boldsymbol{\varepsilon}^{re}) + \Psi^h(\boldsymbol{\xi}^h)$ and of the total generalized strain measure $\boldsymbol{\varepsilon}^r = \boldsymbol{\varepsilon}^{re} + \boldsymbol{\varepsilon}^{r\Delta}$, where $\boldsymbol{\xi}^h$ is strain-like internal hardening variable. Similar to usual stress, one can define hardening-stress and tangent matrix $\boldsymbol{q}^h \coloneqq -\Psi^h_{,\boldsymbol{\xi}^h}$ and $\boldsymbol{K}^h \coloneqq -\Psi^h_{,\boldsymbol{\xi}^h \partial \boldsymbol{\xi}^h}$.

Further assuming a linear hardening constitutive equation, with a diagonal hardening tangent matrix, one can write simply $\boldsymbol{K}^h = \mathrm{diag}(K_1^h \ldots . K_8^h)$ and $\boldsymbol{q}_h = -\boldsymbol{K}^h \boldsymbol{\xi}^h$. Here, two yield function alternatives are presented: independent stress resultant formula $\boldsymbol{\phi}^{(1)}$ and interaction formula $\boldsymbol{\phi}^{(2)}$

$$\begin{aligned} \boldsymbol{\phi}^{(1)} &= \left[\phi_1^{(1)} \ldots \phi_8^{(1)}\right]^T, \text{with } \phi_i^{(1)} = |\sigma_i^r| - \left(\sigma_i^y - q_i^h\right), \\ \boldsymbol{\phi}^{(2)} &= \left[\phi^{(2)}\right], \text{ with } \phi^2 = \textstyle\sum_{i=1,8} {s_i}^2 - 1 \text{ and } s_i = \frac{|\sigma_i^r|}{\sigma_i^y - q_i^h}, \end{aligned} \tag{4}$$

where σ_i^y $(i = 1{,}8)$ are the initial-yield stress-resultants for *pure* stress-resultants configurations (pure tension, pure compression, pure bending, etc.). Plastic flow equations are derived from the maximum plastic dissipation principle, for a dissipation $D = \boldsymbol{\sigma}^r \cdot \dot{\boldsymbol{\varepsilon}}^r - \dot{\Psi}$, subjected to constraints given by the set of yield functions $\boldsymbol{\phi}$. By employing the Lagrange multipliers method, with multipliers $\dot{\boldsymbol{\gamma}}$, with KKT conditions $\gamma_i \geq 0$, $\gamma_i \phi_i = 0$ and $\phi_i \leq 0$, along with consistent plastic flow condition $\gamma_i \dot{\phi}_i = 0$ associated to , it can be restated as a unconstrained optimization problem. Thus, the problem to be solved is, given $\mathcal{L}(\dot{\boldsymbol{\gamma}}, \boldsymbol{\sigma}^r, \boldsymbol{q}^h) = -D + \dot{\boldsymbol{\gamma}} \cdot \boldsymbol{\phi}(\boldsymbol{\sigma}^r, \boldsymbol{q}^h)$, $\min_{\dot{\boldsymbol{\gamma}}, \boldsymbol{\sigma}^r, \boldsymbol{q}^h} (\mathcal{L})$, $\gamma_i \geq 0$, $\gamma_i \phi_i = 0$, $\phi_i \leq 0$. The complete mechanical problem is solved in a staggered procedure (operator split, see Ibrahimbegovic [22], [23]), which requires a local phase computation for finding $\dot{\boldsymbol{\gamma}}, \boldsymbol{\sigma}^r, \boldsymbol{q}^h$ in the plastic process, and a global procedure that renders the consistent elastoplastic modulus $\boldsymbol{D}^{ep}$, that must be used instead of usual $\boldsymbol{D}$ from elastic computation when plasticity is progressing.

In order to complete the description of the model, one must know, besides the usual elastic parameters, the hardening parameters K_i^h and σ_i^y. This is when idea from Dujc [19] is employed: first, build pure stress-state micro-level models with refined 3D finite strain solid or shell elements capable of handling plastic hardening, with a representative length L_{ref}. Then, increase load/displacement, taking note of the load level in which a) yielding begins (characterizing the initial-yield σ_i^y) and b) a limit-point is found (characterizing the ultimate load σ_i^u). Lastly, compute K_i^h so that the plastic work E_p performed between σ_i^y and σ_i^u in micro-scale simulations matches the one for the chosen hardening law for macro-level, assuming that macro-scale also shares the same values of σ_i^y and σ_i^u.

$$K_i^h = \frac{{\sigma_i^u}^2 - {\sigma_i^y}^2}{2E_p} L_{ref} \tag{5}$$

In the upcoming journal paper, several cases were tested for a given cross-sectional shape, and it was notable

the accuracy of the proposed framework, even for complex cases. In Fig. 2, one test example is shown, having a full-scale Ansys Shell 181 element solution as reference. Moreover, it was accessed the important of using a yield function with proper stress coupling, being evident that the simplistic $\boldsymbol{\phi}^{(1)}$ tends to dangerously underestimate critical loads for strongly coupled stresses in plasticity. In Fig. 3, it becomes conspicuous how local bending effects, altogether with plasticity evolution, plays a crucial role in the global cross-sectional behaviour, and, in Fig. 4, it can be seen the robustness of the proposed approach to capture such complex structural pattern.

4.2 Weak multiscale coupling: homogenization

This approach consists in assuming that, a scale separation exists in such a way that it is possible to evaluate stress/strain and energy in the macro-scale integration points by constructing micro-scale mesh of a representative volume element (RVE), apply boundary conditions at this micro-model that corresponds to the actual macro-scale stress/strains in an average sense. This can be done either at runtime, or in a pre-processing phase, in which several cases are tested and approximations of the internal energy function are determined to be directly used during macro-level computation.

A formulation using the latter is under implementation for the elastic case: assuming a macro-level rod model as the one from section 2 . Micro-scale simulations are performed to obtain total internal energy Ψ^e. Calculating the equivalent generalized rod strains at the rod integration point, one can build a function approximation for Ψ^e as function of $\boldsymbol{\varepsilon}^r$. Afterwards, once function Ψ^e becomes known, the expressions that are derived from Kassab and Campello [8] can be directly employed, by using the definitions from eq. (2). In practice, several simulations using finite strain solid elements are needed, with an RVE equivalent to a whole finite rod element are performed, imposing various generalized rod displacements, and a Deep Neural Network is trained to this task. Currently, the first batch of training values from micro-scale simulation is being generated.

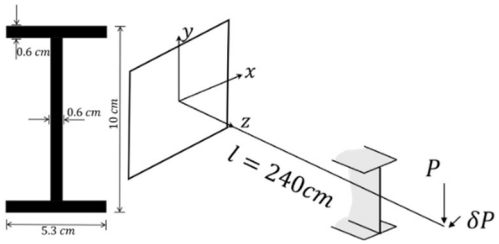

Figure 2. Geometric characterization of the stress-resultant-based elastoplastic rod model (ex. 4.2).

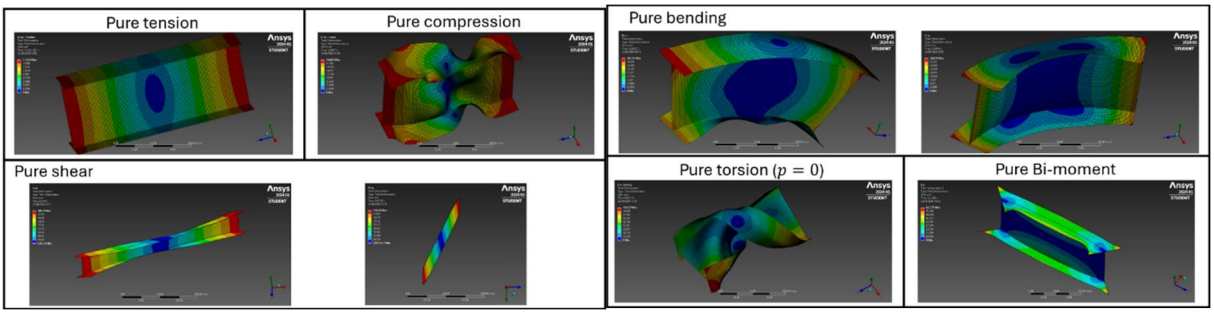

Figure 3. Micro-scale simulations for plastic parameter estimation.

4.3 Strongly coupled multiscale

The last technique that is discussed here is the strongly multiscale approach. In this context, both macro and micro-level meshes coexist in the complete domain of the problem, sharing *interface* nodes. Solution is carried out in a staggered manner, in which for the best iterative guess of displacements of the macro-scale DOFs, micro-scale meshes are solved by imposing either stress or displacements, and both residual and tangent stiffness are calculated by static condensation of the micro-level linearized equilibrium equation. This approach is technically viable and

robust but would not decrease the total amount of degrees of freedom of reticulated structures, since the amount of interface nodes is small (only at the edges of the rod element). Therefore, it has been left aside on behalf of the developments from section 3 , 4.1 and 4.2.

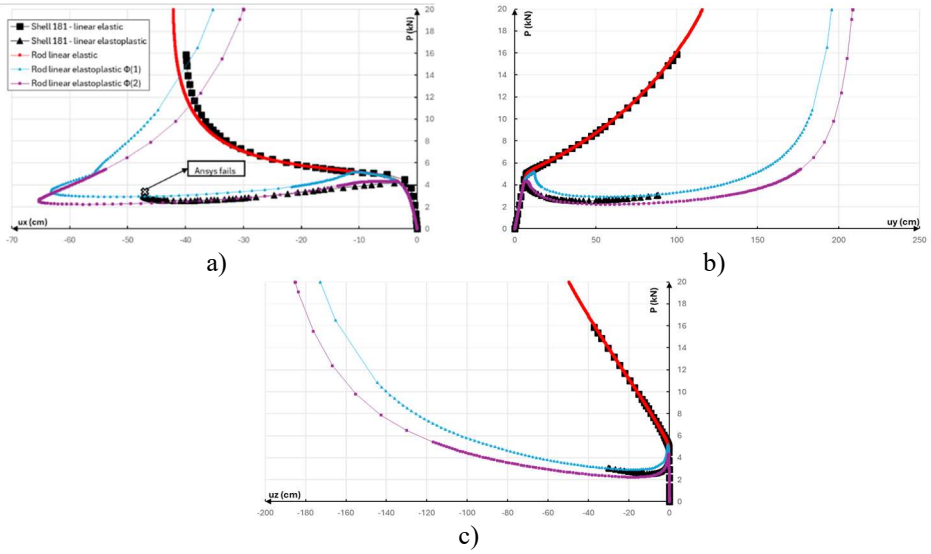

Figure 4. Displacements at the free end of the ex. 4.2. a) Lateral, b) vertical and c) axial displacements

5 Conclusion

We have displayed several alternatives for simulating local effects in thin-walled rod models. From previous experience, it was clear that there was space for development of ROMs with robust capabilities, and that both geometrical and material (e.g., plastic) local effects are pivotal to correctly ascertain structural capacity. Different approaches were shown, from frameworks that were already developed and successfully tested, to works in development or even to conceptual insights with potential to be tested in the near future. We hope to be able to present some of these results during the conference.

Acknowledgements. This work was supported by FAPESP (Sao Paulo State Research Foundation), Brazil, under the grants 2023/16272-1 and 2022/15644-0, and CNPq (Conselho Nacional de Desenvolvimento Científico e Tecnológico), Brazil, under the grants 313046/2021-2 and 308142/2018-7, as well as by ANR (Agence Nationale Recherche) in France under the grant ANR-20-CE46-0012-01 and IUF (Institut Universitaire France) under grant 1479. The opinions, hypotheses, conclusions and recommendations expressed herein are the sole responsibility of the authors and do not necessarily reflect the funding agencies visions. Screenshots of shell models are used as courtesy of ANSYS, Inc.

Authorship statement. The authors hereby confirm that they are the sole liable persons responsible for the authorship of this work, and that all material that has been herein included as part of the present paper is either the property (and authorship) of the authors, or has the permission of the owners to be included here.

References

[1] J. C. Simo, “A finite strain beam formulation. The three-dimensional dynamic problem. Part I,” *Comput Methods Appl Mech Eng*, vol. 49, no. 1, pp. 55–70, May 1985, doi: 10.1016/0045-7825(85)90050-7.

[2] J. C. Simo and L. Vu-Quoc, “A three-dimensional finite-strain rod model. part II: Computational aspects,” *Comput Methods Appl Mech Eng*, vol. 58, no. 1, pp. 79–116, Oct. 1986, doi: 10.1016/0045-7825(86)90079-4.

[3] A. Ibrahimbegović, F. Frey, and I. Kožar, "Computational aspects of vector-like parametrization of three-dimensional finite rotations," *Int J Numer Methods Eng*, vol. 38, no. 21, pp. 3653–3673, Nov. 1995, doi: 10.1002/nme.1620382107.

[4] A. Ibrahimbegović and F. Frey, "Finite element analysis of linear and non-linear planar deformations of elastic initially curved beams," *Int J Numer Methods Eng*, vol. 36, no. 19, pp. 3239–3258, Oct. 1993, doi: 10.1002/nme.1620361903.

[5] P. M. Pimenta and T. Yojo, "Geometrically Exact Analysis of Spatial Frames," *Appl Mech Rev*, vol. 46, no. 11S, pp. S118–S128, Nov. 1993, doi: 10.1115/1.3122626.

[6] P. M. Pimenta and E. M. B. Campello, "Geometrically nonlinear analysis of thin-walled space frames," Proceedings of the II ECCM (European Conference on Computational Mechanics), 2001, p. 20.

[7] E. M. B. Campello and L. B. Lago, "Effect of higher order constitutive terms on the elastic buckling of thin-walled rods," *Thin-Walled Structures*, vol. 77, pp. 8–16, Apr. 2014, doi: 10.1016/j.tws.2013.11.001.

[8] M. P. Kassab, E. M. B. Campello, and P. M. Pimenta, "Advances on kinematically exact rod models for thin-walled open-section members: Consistent warping function and nonlinear constitutive equation," *Comput Methods Appl Mech Eng*, vol. 407, p. 115933, Mar. 2023, doi: 10.1016/j.cma.2023.115933.

[9] C. da Costa e Silva, S. F. Maassen, P. M. Pimenta, and J. Schröder, "A simple finite element for the geometrically exact analysis of Bernoulli–Euler rods," *Comput Mech*, vol. 65, no. 4, pp. 905–923, Apr. 2020, doi: 10.1007/s00466-019-01800-5.

[10] M. A. Crisfield, "A consistent co-rotational formulation for non-linear, three-dimensional, beam-elements," *Comput Methods Appl Mech Eng*, vol. 81, no. 2, pp. 131–150, Aug. 1990, doi: 10.1016/0045-7825(90)90106-V.

[11] F. Gruttmann, R. Sauer, and W. Wagner, "A geometrical nonlinear eccentric 3D-beam element with arbitrary cross-sections," *Comput Methods Appl Mech Eng*, vol. 160, no. 3–4, pp. 383–400, Jul. 1998, doi: 10.1016/S0045-7825(97)00305-8.

[12] F. Gruttmann, R. Sauer, and W. Wagner, "Theory and numerics of three–dimensional beams with elastoplastic material behaviour," *Int J Numer Methods Eng*, p. 33, 2000, doi: 10.1002/1097-0207(20000830)48:123.0.CO;2-6.

[13] R. Gonçalves, "An assessment of the lateral-torsional buckling and post-buckling behaviour of steel I-section beams using a geometrically exact beam finite element," *Thin-Walled Structures*, vol. 143, p. 106222, Oct. 2019, doi: 10.1016/j.tws.2019.106222.

[14] E. R. Dasambiagio, P. M. Pimenta, and E. M. B. Campello, "A finite strain rod model that incorporates general cross section deformation and its implementation by the Finite Element Method," in *Mechanics of Solids in Brazil 2009*, 1st ed., vol. 1, H. S. da Costa Mattos and M. Alves, Eds., Rio de Janeiro: Brazilian Society of Mechanical Sciences and Engineering, 2009, pp. 145–168.

[15] P. M. Pimenta and E. M. B. Campello, "A fully nonlinear multi-parameter rod model incorporating general cross-sectional in-plane changes and out-of-plane warping," *Latin American Journal of Solids and Structures*, vol. 1, no. 1, pp. 119–140, 2003.

[16] R. Schardt, "Generalized beam theory—an adequate method for coupled stability problems," *Thin-Walled Structures*, vol. 19, no. 2–4, pp. 161–180, Jan. 1994, doi: 10.1016/0263-8231(94)90027-2.

[17] R. Gonçalves, M. Ritto-Corrêa, and D. Camotim, "A large displacement and finite rotation thin-walled beam formulation including cross-section deformation," *Comput Methods Appl Mech Eng*, vol. 199, no. 23–24, pp. 1627–1643, Apr. 2010, doi: 10.1016/j.cma.2010.01.006.

[18] R. Bebiano, D. Camotim, and R. Gonçalves, "GBTul 2.0 − A second-generation code for the GBT-based buckling and vibration analysis of thin-walled members," *Thin-Walled Structures*, vol. 124, pp. 235–257, Mar. 2018, doi: 10.1016/j.tws.2017.12.002.

[19] J. Dujc, B. Brank, and A. Ibrahimbegovic, "Multi-scale computational model for failure analysis of metal frames that includes softening and local buckling," *Comput Methods Appl Mech Eng*, vol. 199, no. 21–22, pp. 1371–1385, Apr. 2010, doi: 10.1016/j.cma.2009.09.003.

[20] A. Ibrahimbegovic, R. Mejia-Nava, and S. Ljukovac, "Reduced model for fracture of geometrically exact planar beam: Non-local variational formulation, ED-FEM approximation and operator split solution," *Int J Numer Methods Eng*, vol. 125, no. 1, Jan. 2024, doi: 10.1002/nme.7369.

[21] S. Ljukovac, A. Ibrahimbegovic, R.-A. Mejia-Nava, and I. Imamovic, "Geometrically exact 3D beam theory with embedded strong discontinuities for modeling of localized failure in bending," *Int J Solids Struct*, vol. 297, p. 112850, Jul. 2024, doi: 10.1016/j.ijsolstr.2024.112850.

[22] A. Ibrahimbegovic, *Nonlinear Solid Mechanics*, vol. 160. Dordrecht: Springer Netherlands, 2009. doi: 10.1007/978-90-481-2331-5.

[23] A. Ibrahimbegović and F. Frey, "An efficient implementation of stress resultant plasticity in analysis of Reissner-Mindlin plates," *Int J Numer Methods Eng*, vol. 36, no. 2, pp. 303–320, Jan. 1993, doi: 10.1002/nme.1620360209.